Computational Materials Science 79 (2013) 125–131

Contents lists available at SciVerse ScienceDirect

Computational Materials Science

journal homepage: www.elsevier.com/locate/commatsci

Energy band gap and optical properties of lithium niobate from ab initio calculations

S. Mamoun [a], A.E. Merad [b,*], L. Guilbert [a]

[a] Université de Lorraine, Laboratoire Matériaux Optiques, Photonique et Systèmes (LMOPS), EA 4423, 2 rue Edouard Belin, 57070 Metz, France
[b] Equipe: Physique de L'état Solide, Laboratoire de Physique Théorique (LPT), Université de Tlemcen, Algeria

ARTICLE INFO

Article history:
Received 24 December 2012
Received in revised form 30 May 2013
Accepted 1 June 2013
Available online 5 July 2013

Keywords:
DFT calculations
Lithium niobate
Electronic properties
Optical properties

ABSTRACT

The electronic and optical properties of stoichiometric lithium niobate are calculated from first principles within the Generalized Gradient Approximation (GGA). The band gap is found slightly indirect. Its value, underestimated by the GGA, is corrected on the basis of the refractive index by using our new approach called *reverse scissor correction* procedure. The corrected value (4.9 eV) is fairly comparable to previous ones obtained by GW calculation. The frequency dispersions of the dielectric function are re-calculated for different scissor corrections and compared to the experimental Sellmeier equation. A good agreement is obtained in the NIR-VIS-NUV range with our corrected band gap. The hopping integrals and effective masses at the extrema of the conduction and valence bands are also estimated.

1. Introduction

Lithium niobate ($LiNbO_3$, LN) has attracted major interest over more than 30 years, since the discovery of the bulk photovoltaic effect in this material [1]. The very strong photorefraction induced by this effect has been extensively studied, owing to its specific applications (holographic storage, spatial solitons) or to its drawbacks in other applications (frequency conversion, electro-optical modulation). The high concentration of niobium antisite defects in congruent material, which plays a major role in optical properties, can be reduced by charge compensation (e.g. by Mg doping) or by shifting the intrinsic composition near stoichiometry. Structural, mechanical, electrical, and optical properties of congruent (CLN) and nearly stoichiometric (NSLN) crystals and their applications are compiled in several publications, namely the most often cited review paper [2] and books [3–6].

By first-principle calculations based on the Density Functional Theory (DFT) [7], Inbar and Cohen [8] have explained the origin of ferroelectricity in LN. Kohiki et al. [9] have compared the theoretical electron energy loss function to the experimental ones based on X-ray photoemission spectra. Other works have been devoted to phonon calculations [10,11]. As far as electronic and optical properties are concerned, different approximations and related methods within DFT have been used. So, different values of the energy band gap have been proposed for stoichiometric LN (SLN) in ferroelectric phase. Let us classify chronologically the available results. The Local Density Approximation (LDA) gave: 2.62 eV [12], 3.1 eV [8], 3.48 eV [13], 3.52 eV [14] and 3.35 eV [15]. The Generalized Gradient Approximation (GGA) results are: 3.50 eV [13], 3.48 eV [16], 3.61 eV [17] and 3.32 eV [18]. Other corrected values to the LDA have been also proposed: Ching et al. applied an approximate self-energy correction to their LDA result (2.62 eV) and found a direct gap of 3.56 eV [12], whereas Nahm and Park found 3.59 eV by introducing the Hubbard correction (LDA + *U*) [15].

As a rule, LDA and GGA methods are known to give underestimated values of the band gap, owing to the fact that they do not involve excited states. The underestimation can amount to 50% compared to experimental data [19,20] and is roughly proportional to the band gap [21], thus the absolute error is larger for insulators than for semiconductors. On another hand, it is worth noticing that all papers cited above have compared the theoretical values obtained for the band gap to a so-called 'experimental' one (3.78 eV) deduced by extrapolating a straight-line fit of the absorption function $\alpha^{1/2}$ versus photon energy [22]. This simple procedure, usually valid for small gap semiconductors, becomes rough for higher gaps [23] and is thus highly questionable for insulators. Moreover, all above-cited ab initio results concern pure, perfectly stoichiometric LN (SLN); any NSLN sample deviates more or less from this ideal case, and it is known that residual intrinsic defects

* Corresponding author. Address: Group: Solid State Physics, Theoretical Physics Laboratory (LPT), Physics Department, Faculty of Sciences, A Belkaïd University, Box. 119, Tlemcen 13000, Algeria. Tel./fax: +213 43 28 63 08.
E-mail addresses: aemerad@gmail.com, k_merad@mail.univ-tlemcen.dz (A.E. Merad).

0927-0256/$ - see front matter © 2013 Elsevier B.V. All rights reserved.
http://dx.doi.org/10.1016/j.commatsci.2013.06.017

(Li vacancies and Nb antisites) induce a significant red-shift on the absorption edge [15,22]. Recently, the proposed band gap obtained by GW approximation (self-energy expansion in terms of single-particle Green's function G and screened Coulomb interaction W) has been suggested to be more than 1 eV higher compared to the experimental one frequently cited in the literature (3.78 eV). The obtained energy band gap values by Schmidt et al. [16] and Thierfelder et al. [17] are 5.37 eV and 4.7 eV respectively.

In view of the large scattering in the theoretical estimates reported for the band gap of SLN, we may conclude that this important parameter is still ill-defined. Therefore, we aim to tackle this problem from a different approach, essentially based on the dielectric response and the 'scissor' operator. This operator is an empirical correction which can be applied to both LDA and GGA underestimated band gaps; basically, it consists in shifting the band energies and keeping their dispersions unchanged [24]. It is thus a rigid-band approximation, through which the band gap is just enlarged with a constant potential in order to reproduce the experimental value. It is commonly used for semiconductors [25]. The originality of our method is to apply this procedure in order to reproduce the value of the refractive index in SLN, which is in principle well-known [26] and certainly more reliable than the experimental value of the band gap based on the absorption spectrum [22], on which most of the theoretical corrections have been based in previous works. We perform here the calculation with different scissor shifts until the low-frequency value of the refractive index of SLN is obtained; then we re-calculate the dispersions of the ordinary and extraordinary refractive indices and compare it to the experimental Sellmeier equation [26] and complementary index data [27]. We also investigate the optical properties obtained with the scissor shifts corresponding to the experimental value of the band gap (3.78 eV) and the theoretical GW one (4.71 eV), in order to make a comparative analysis.

2. Computational considerations

Calculations are performed using the full-potential linear augmented plane-wave method (FP-LAPW) [28,29] implemented in the Wien2k code [30,31] which self-consistently, finds the eingenvalues and eingenfunction of the Kohn–Sham [32] equations for the system. We use the Generalized Gradient Approximation (GGA) as parameterized by Perdew et al. [33], which includes the second order gradient components. The core states of Li, Nb and O atoms are self-consistently treated and relativistically-relaxed in a spherical approximation, whereas the valence states are treated self-consistently within the semi-relativistic approximation (spin–orbit coupling excluded). The valence electron configurations used in the calculations are: Li($2s^1$), Nb($4d^3 5s^2$) and O($2s^2 2p^4$). The wave function, charge density and potential are expanded by spherical harmonic functions inside non-overlapping spheres surrounding the atomic sites (muffin-tin spheres) and by a plane-wave basis set in the remaining space of the unit cell (interstitial region). The maximum l quantum number for the wave function expansion inside atomic spheres is confined to $l_{max} = 10$. The charge density is Fourier-expanded up to $G_{max} = 9.5$ $(\text{Ry})^{1/2}$. The convergence parameter $R_{MT}K_{max}$ which controls the size of the basis set in these calculations is set to 7 (K_{max} is the maximum modulus for the reciprocal lattice vector and R_{MT} is the average radius of the muffin tin spheres). The muffin-tin radius values for Li, Nb and O were chosen at 1.94, 1.88 and 1.67 atomic units (a.u.) respectively. For the calculation of electronic and optical properties respectively, the reciprocal space is sampled by a $4 \times 4 \times 4$ (resp. $11 \times 11 \times 11$) Monkhorst–Pack mesh [34] with 13 (resp. 146) k-vectors in the irreducible Brillouin zone. This sampling is found sufficient to have good results as it is shown also in the works cited above [8,10,13,15–17], therefore it is adopted here to keep the comparability. 2000 plane waves with no inversion are generated. The iterative process is repeated until the calculated total energy of the crystal converges to less than 10^{-4} Ry. The experimental structural parameters and positions used for the calculation are these of Ref. [35]. The rhombohedral unit cell of the ferroelectric structure contains two molecules $LiNbO_3$ (10 atoms) as illustrated in Fig. 1.

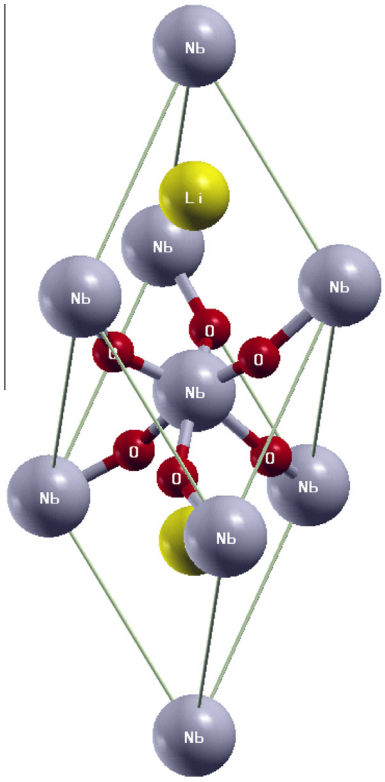

Fig. 1. Primitive unit cell of the ferroelectric lithium niobate.

3. Principle of the scissor correction

The scissor correction is commonly used when an underestimated value of the band gap is obtained within DFT methods [36]. The offset of the gap can be chosen with respect to either a theoretical value determined more accurately by GW calculation [37,38] or an experimental value deduced from optical measurements [39,40]. It consists in a modification of the Khon–Sham – LDA/GGA Hamiltonian, by an additional term that rigidly shifts the conduction band up in energy [41]. The scissor operator $\hat{S}$ is given by [42]:

$$\hat{S} = \hbar\bar{\omega}\sum_n \int d^3k(1 - f_n)|nk\rangle\langle nk| \tag{1}$$

In Eq. (1), $\hbar\bar{\omega}$ is the energy correction to be applied, f_n is the k-independent occupation factor equal to one for occupied states and zero for unoccupied states, $|nk\rangle$ is a ket with coordinate representation $\Psi_{nk}(r) = \langle n|nk\rangle$. The total Hamiltonian with the scissor correction is thus:

$$H^S\left(r, \frac{\hbar}{i}\nabla\right) = H^{GGA}\left(r, \frac{\hbar}{i}\nabla\right) + S\left(r, \frac{\hbar}{i}\nabla\right) \tag{2}$$

The eigenstates of $H^s(r, \frac{\hbar}{i}\Delta)$ and $H^{GGA}(r, \frac{\hbar}{i}\Delta)$ are identical, but the eigenvalues are different, so that:

$$H^{GGA}\left(r,\frac{\hbar}{i}\nabla\right)\Psi_{nk}(r)=\hbar\omega_{nk}^{GGA}\Psi_{nk}(r) \quad (3)$$

$$H^{S}\left(r,\frac{\hbar}{i}\nabla\right)\Psi_{nk}(r)=\hbar\omega_{nk}^{S}\Psi_{nk}(r) \quad (4)$$

$$\omega_{nk}^{S}=\omega_{nk}^{GGA}+(1-f_n)\bar{\omega} \quad (5)$$

4. Results and discussions

4.1. Band structure and densities of states

The selected high-symmetry points and directions of the hexagonal Brillouin zone are shown in Fig. 2. We have calculated the electronic dispersions along these points then the total density of states (TDOS) shown in Fig. 3. The valence and conduction bands (VB, CB) are formed by packs of several bands. The origin of the energies is taken at the top of the upper VB (UVB). The GGA energy gap is found to be slightly indirect, with a minimum of the lower CB (LCB) on the ΓK segment; its value is E_g = 3.487 eV (the direct band gap at Γ point is 3.50 eV). This result is in fair agreement with previous ones obtained by LDA (3.35 eV) [15] or by GGA: 3.48 eV [16], 3.32 eV [18] (see Table 1).

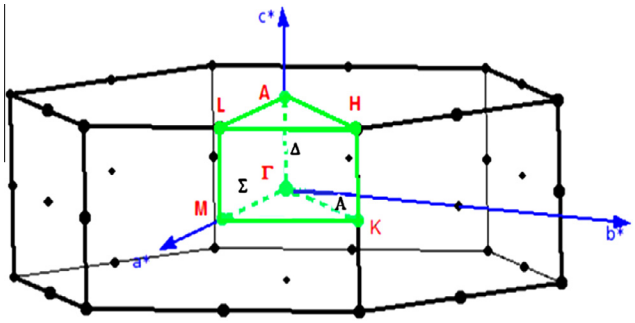

Fig. 2. Selected high symmetry points: Γ, M, K, A, L and H for the irreducible Brillouin zone; Σ, Λ, and Λ are the high symmetry directions linked these points.

In order to assign the separate groups of bands of the TDOS to specific atomic levels, we have plotted in Fig. 4 the partial densities of states (PDOS) for Li, Nb and O atoms. The LCB mainly consists in the Nb-4*d* manifold and is 2.15 eV wide. It is separated from the next CB by a gap of 1.71 eV. The UVB, 4.57 eV in width, is a mixture of O-2*p* and Nb-4*d* orbitals indicating that the Nb–O bond is partly covalent. It is separated from the O-2*s* level (1.99 eV wide) by a gap of 10.42 eV. Contrarily to what has been reported in Ref. [8] the deep VB located at about −30 eV is made of Nb-4*p* states and not of Li-2*s* states. We find that Li-2*s* states form an upper CB located at +13.8 eV, in agreement with the results of Kohiki et al. [9]. This confirms the affirmation first given by Inbar and Cohen [8] then relayed by Veithen and Ghosez [13] that Li atoms completely loose their 2*s* electron and do not participate to the covalence (i.e. fully ionized and form an ionic bond with the rest of the crystal).

The hopping integrals are obtained from the widths of the LCB and the UVB. For the former (between niobium atoms) we find J_{Nb} = 34.6 meV, in excellent agreement with the value of 35 meV previously reported [22]. For the latter (between oxygen atoms) we find J_O = 17.8 meV. No available data of J_O has been found for comparison.

The corresponding effective masses are obtained from the expression:

$$m^{*}=\pm\hbar^{2}\left(\frac{d^{2}E_k}{dk^{2}}\right)^{-1} \quad (6)$$

The effective masses of holes m_h^* and electrons m_e^* are hence estimated, respectively at the UVB maximum which occurs at Γ point, and at the LCB minimum found on the ΓK segment (at 0.8867 nm^{-1} from Γ). The obtained values (in unit of free electron mass m_0) are m_h^* = 3.187 and m_e^* = 4.26. The latter takes into account the presence of six equivalent minima owing to hexagonal symmetry.

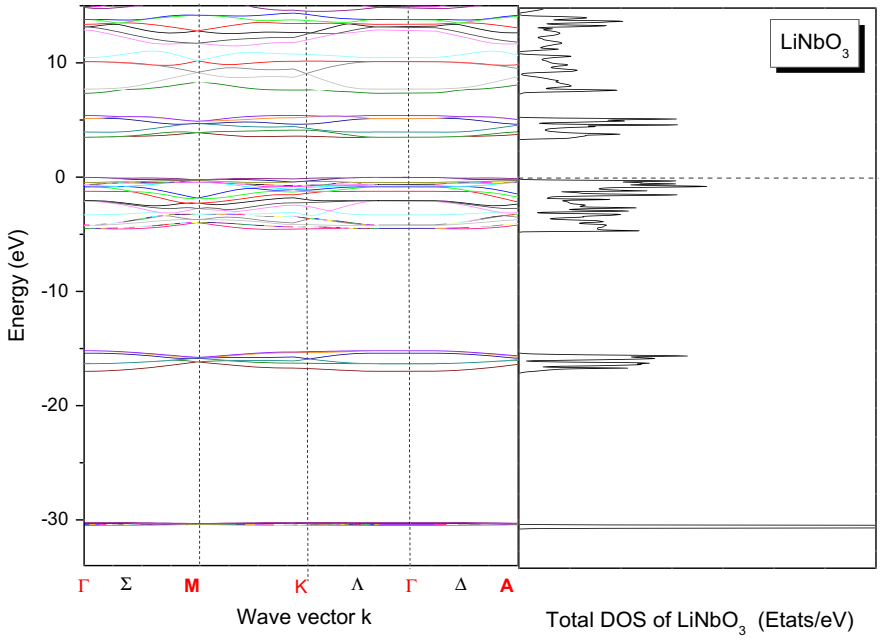

Fig. 3. DFT–GGA band gap structure of ferroelectric lithium niobate obtained along the high symmetry direction chosen in the Brillouin zone (left) and the calculated total density of states (right). The energy scale is in eV and the VBM is chosen as energy zero.

Table 1
Energy band gap, static real part of the dielectric function and the refractive index given in the *xx* and *zz* directions, and their average values. All refractive indices are calculated at $T = 0$ K excepted the experimental ones.

	Previous theoretical calculations				Exp	Our results			
	LDA	Corrected LDA	GGA	GW		Without correction	With scissor correction		
E_g	2.62[a]	3.56[a]	3.32[b], 3.48[c]	4.71[d], 5.37[c]	3.78[e]	3.487	3.78[e]	4.71[d]	4.90
$\varepsilon_1(\omega = 0)_{xx}$	–	–	5.91[b]	–	–	5.42	5.50	4.95	4.85
$\varepsilon_1(\omega = 0)_{zz}$	–	–	5.63[b]	–	–	5.27	5.08	4.59	4.50
$\varepsilon_1(\omega = 0)$	6.57[a]	4.91[a]	5.82[b]	–	–	5.56	5.36	4.83	4.73
n_o	–	–	2.43[b]	–	2.21[f], 2.23[g]	2.39	2.34	2.22	2.20
n_e	–	–	2.37[b]	–	2.12[f], 2.15[g], 2.14[h]	2.29	2.25	2.14	2.12

[a] Ref. [12].
[b] Ref. [18].
[c] Ref. [16].
[d] GW calculation, Ref. [17].
[e] Experimental value deduced from the absorption coefficient, Ref. [22].
[f] Values obtained from the Sellmeier equation using the parameters of Ref. [26] (calculated at $\omega = 0$ and $T = 0$ K for SLN).
[g] Values obtained at $\lambda = 1064$ nm, at room temperature for rich lithium LN. Ref. [27].
[h] Value obtained at $\lambda = 1200$ nm, at $T = 24.5°$ and for LN in a composition of 49.9 mol% Li_2O. Ref. [26].

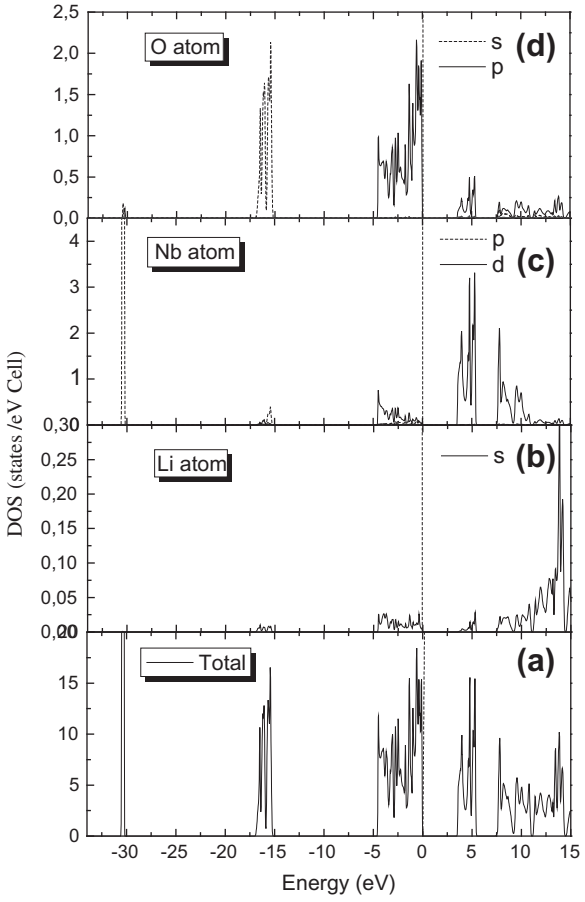

Fig. 4. (a) Total density of state for $LiNbO_3$ in its ferroelectric phase. (b) Partial density of states for Li. (c) Partial density of states for Nb. (d) Partial density of states for O.

4.2. Scissor correction application

The scissor operator is commonly used to deduce the corrected optical properties from the shifted band gap. In this work, we use a "*reverse*" method: we take the refractive index at low frequency as a target and seek the band gap correction which reproduces this index value. Then we follow the direct method to calculate the corrected dispersions of the dielectric function (real and imaginary part) and refractive indices. We base our calculation on the general expression of the complex dielectric tensor [43]. The imaginary part $\varepsilon_2(\omega)$ involves all transitions from occupied to unoccupied states:

$$\varepsilon_2(\omega)_{\alpha\beta} = \frac{4\pi^2 e^2}{m^2\omega^2}\sum_{i,f}\int \langle f|p_\alpha|i\rangle\langle i|p_\beta|f\rangle W_i(1-W_f)\delta(E_f - E_i - \hbar\omega)d^3k \quad (7)$$

In Eq. (7), $\langle f|p_\alpha|i\rangle$ and $\langle i|p_\beta|f\rangle$ are dipole matrix elements, f and i are final and the initial states respectively, W_i (resp. W_f) is the Fermi distribution function centred at E_i (resp. E_f).

The real part $\varepsilon_1(\omega)$ is computed from $\varepsilon_2(\omega)$ using the Kramers–Kronig relation in the form:

$$\varepsilon_1(\omega)_{\alpha\alpha} = 1 + \frac{2}{\pi}p\int_0^\infty \frac{\omega'\varepsilon_2(\omega')_{\alpha\alpha}}{\omega'^2 - \omega^2}d\omega' \quad (8)$$

In Eq. (8), P means the principal value of the integral. Finally, the real part of the refractive index is expressed as function of the complex dielectric function $\tilde{\varepsilon}(\omega)_{\alpha\alpha}$ by:

$$n(\omega)_{\alpha\alpha} = \sqrt{\frac{|\varepsilon(\omega)_{\alpha\alpha}| + \varepsilon_1(\omega)_{\alpha\alpha}}{2}} \quad (9)$$

The dielectric function is calculated by Eqs. (7) and (8) with our raw GGA value of the band gap (simple solid line (red)) and with different scissor shifts (dot, dashed and thick solid lines (black)) (see Fig. 5). As expected, the effect of the scissor correction on the imaginary part is basically a rigid shift of the dispersions towards higher energies. The real part is not only shifted but also significantly decreased at low frequencies. The value of the extraordinary index obtained at $\omega = 0$ without scissor correction is $n_e = 2.29$, significantly larger than the value obtained by extrapolating the Sellmeier equation [26] at $\omega = 0$, $T = 0$ K ($n_e = 2.12$). In order to get the corrected band gap, we re-evaluate the refractive index $n_e(\omega = 0)$ for different scissor shifts $\Delta E = \hbar\bar{\omega}$ by using Eq. (8), until the target value 2.12 is found. Finally we obtain $\Delta E = 1.41$ eV, that is ~40% of our initial GGA value of the band gap, 3.49 eV. Our corrected value of the band gap is thus 4.90 eV, in good agreement with the GW value, 4.71 eV [17]. Thus, our approach with a cheap computation, maintain a comparable level of accuracy to the more sophisticated and expensive GW calculations. Our result thus corroborates the indication that the rigid band gap of SLN could be more than 1 eV larger than the so-called 'experimental' value, 3.78 eV [22]. This large difference is worth being discussed. It has been observed for several materials that GW calculations overestimate the band gap with respect to experimental values [44,45]. This mismatch can be explained as a follows: The electron–phonon coupling is usually strong in polar crystals, and can thus induce a significant reduction of the band

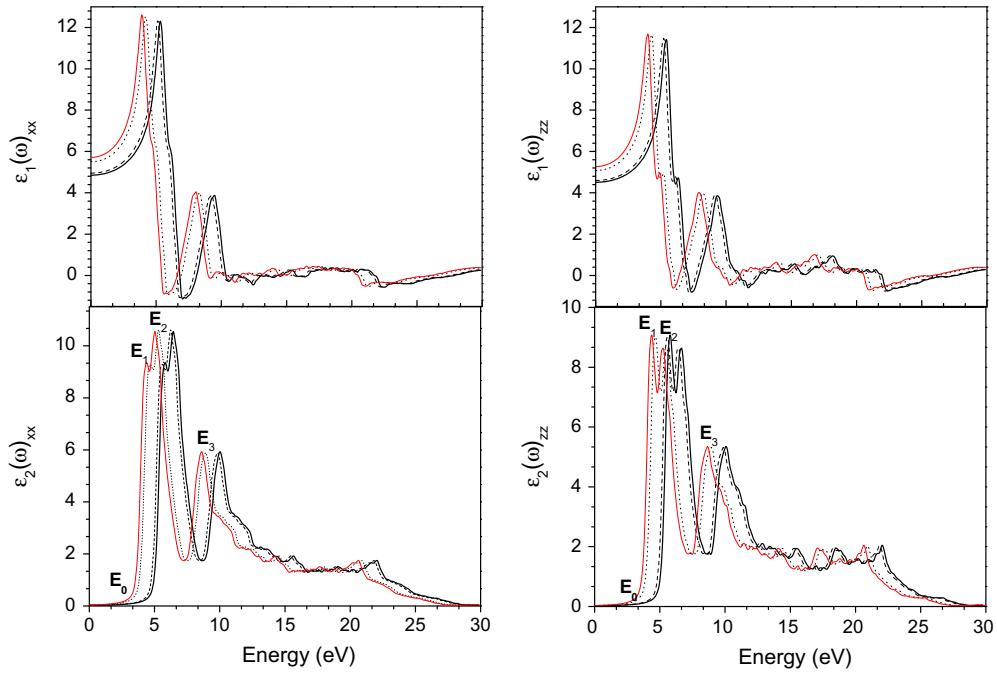

Fig. 5. Calculated real $\varepsilon_1(\omega)$ and imaginary part $\varepsilon_2(\omega)$ of the dielectric function $\varepsilon(\omega)$, of Lithium Niobate in its ferroelectric phase as a function of the photon energy (eV) given in the *xx* direction (left) and in the *zz* direction (right). The simple solid lines (red) represent the raw GGA calculation (3.48 eV). The dot lines refer to the readjusted band gap to the experimental one (3.78 eV) and the dashed lines are the readjusted band gap to the GW results (4.71 eV), while the thick solid lines represent the readjusted one to our predicted energy band gap (4.9 eV). (For interpretation of the references to colour in this figure legend, the reader is referred to the web version of this article.)

gap compared to the rigid value obtained by GW calculation. In the case of LN, it is known that free electrons self-trap into small polarons [46]. In SLN, since point defects are virtually absent, only free polarons can exist; their stabilization energy is estimated by Schirmer et al. to 0.55 eV [46]. The quasi-particle responsible for the lowering of the absorption band in SLN could be an excitonic pair involving a free hole and a free electron polaron. In fact, all available data rely on optical measurements, which do not yield information about the electronic band gap but only about the optical band gap (i.e. to the excitonic level), which might differ by 1 eV or more in compounds with high polarizability such as LN, as explained by Schmidt et al. [16] and Thierfelder et al. [17]. Therefore, in the case of LN or any other polar crystal of strong electron–phonon coupling, the absorption coefficient usually taken as a reference for estimating the band gap is not relevant. This is the reason why we have used the refractive index as a target within our correction procedure.

Applying now the direct procedure with our corrected band gap, we have calculated the interband transitions from the O-2*p* valence bands to the Nb-4*d* conduction bands, namely the absorption peak energies E_0, E_1, E_2 and E_3, in order to compare them to other theoretical values [12]. These peaks are illustrated in the imaginary part of the dielectric function (Fig. 5). The first resonance E_0 is obviously related to the rigid band gap E_g and mainly responsible for the dispersion of the refractive indices in the visible and near UV ranges, addressed in the following section. The raw and corrected values of the permittivity and refractive indices at $\omega = 0$ are compiled in Table 1. The higher resonance energies E_1, E_2 and E_3 are given in Table 2. The minimum E_{min} between E_2 and E_3 is the reflection of the energy gap of about 1.7 eV above the Nb-4*d* conduction band obtained by our GGA calculations as it is also explained in Ref. [12].

4.3. Dispersions of the refractive indices

It is now necessary to check whether the whole dispersions of the refractive indices calculated with various corrected band gap values reproduce the experimental dispersions. We calculate these

Table 2
Main features of the interband optical transitions of the imaginary part of the dielectric function given in both of the *xx* and *zz* directions.

	Our results				Other calculations
	Without correction	With correction			Average values
	GGA	Exp	GW	Predicted	Corrected LDA
xx					
E_1	4.39	4.67	5.59	5.80	5.4[a]
E_2	5.02	5.32	6.24	6.43	–
E_{min}	7.22	7.60	8.53	8.63	7.9[a]
E_3	8.61	8.91	9.84	10.03	9.0[a]
zz					
E_1	4.37	4.67	5.56	5.78	5.4[a]
E_2	5.24	5.48	6.41	6.65	–
E_{min}	7.47	7.77	8.70	8.58	7.9[a]
E_3	8.67	8.94	9.86	10.08	9.0[a]

[a] Ref. [12].

dispersions with scissor shifts corresponding to our corrected value of the gap (4.90 eV) and to the GW value (4.71 eV) recently reported [17]. The results are shown in Fig. 6. Since the calculated dispersions involve only electronic contributions, they have to be compared to the ones deduced from the electronic terms of the Sellmeier equation [26]:

$$n_i^2(\omega) = \frac{A_i}{1 - (\omega/\omega_i)^2} + A_{UV} \tag{10}$$

with $i = o$ (ordinary) or e (extraordinary). The IR term which appears in Ref. [26] has been omitted in Eq. (10), since this term is related to phonon contributions which are not taken into account in DFT calculations. The parameters of Eq. (10) deduced at 0 K from Ref. [26] are: $A_o = 2.11$, $A_e = 1.96$, $\hbar\omega_o = 5.56$, $\hbar\omega_e = 5.68$ and $A_{UV} = 2.6613$ (plasmon contribution). They have been obtained in Ref. [26] by least-square fits on experimental data in the wavelength range 400–1200 nm (1–3 eV); since the electronic

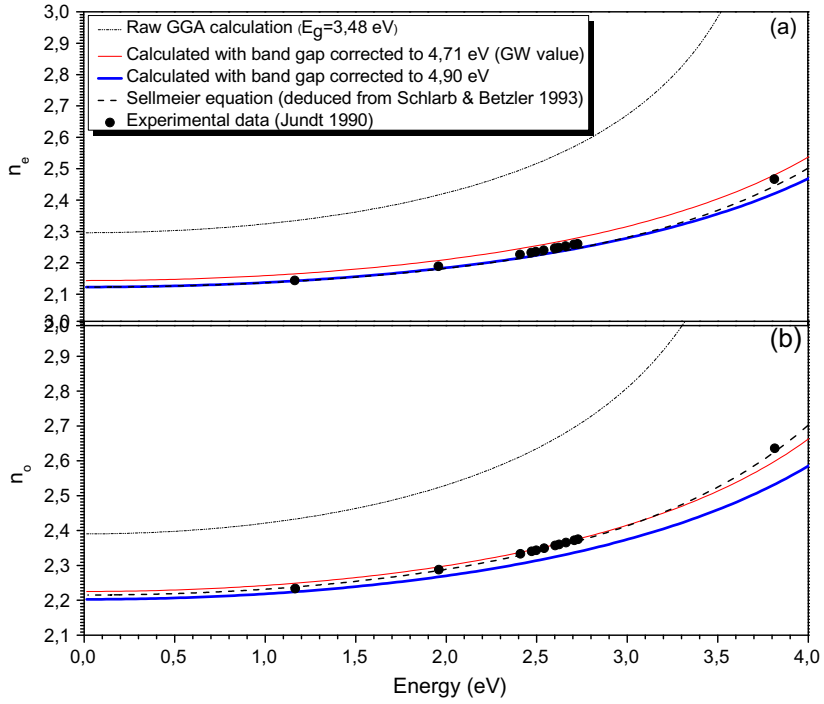

Fig. 6. Dispersions of the extraordinary (a) and ordinary (b) refractive indices at low frequencies. GGA calculation (3.48 eV), correction to the GW band gap (4.71 eV) and correction to our predicted value (4.9 eV) are compared to the Sellmeier equation obtained using the parameters of Scharb and Betzler [26] and the experimental results of Jundt et al. [27].

contributions in both n_o and n_e are quasi constant below 1 eV, we may consider that the comparison between calculated dispersions and Sellmeier ones is relevant in the photon energy range 0–3 eV. Experimental data of Jundt et al. [27] are also reported in Fig. 6. For n_e (Fig. 6a), a better agreement is achieved with our corrected gap (4.90 eV); this is of course not surprising, since this corrected value was obtained by targeting $n_e(\omega = 0)$, but it is worth noticing that the calculated dispersion $n_e(\omega)$ fits well with the Sellmeier equation up to 3.2 eV. For n_o, (Fig. 6b), the agreement is better with the gap corrected to the GW value (4.71 eV). We may thus conclude that the rigid band gap of stoichiometric lithium niobate at 0 K is probably (4.8 ± 0.1) eV. It is difficult to say whether the slight misfits observed in the near UV range (especially on n_o) are due to the approximation inherent to the scissor-corrected GGA method or to the fact that the validity range of the experimental Sellmeier equation is restricted to 3 eV. Since refractive index data in SLN beyond 3 eV are scarce, it may be suggested to complement experimental measurements in the near UV range.

5. Conclusion

In this paper, we have investigated the electronic and optical properties of pure, stoichiometric lithium niobate from first principal calculations. The band structure has been fully described, and the densities of states in the valence and conduction bands have been unambiguously assigned. The results confirm that Li ions do not participate to the covalence and that the optical properties result mainly from transitions between O-2*p* and Nb-4*d* states. By using our *reverse scissor correction* procedure, we have refined the value of the rigid band gap in order to reproduce the experimental value of the refractive index $n_e(\omega = 0)$ and finally the whole dispersions of both indices $n_o(\omega)$ and $n_e(\omega)$ in the photon energy range 0–3 eV. Four important conclusions can be drawn from this study: (i) the experimental value of the band gap (3.78 eV), based only on the absorption spectrum and frequently cited in the literature, is not a relevant comparison parameter for the rigid band gap calculated by any DFT method, owing to the strong electron–phonon interaction in this crystal; (ii) therefore, the apparent agreement between this so-called experimental value and theoretical ones previously obtained by several authors using LDA or GGA methods [8,13–15,18] seems fortuitous and cannot be considered as a criterion of validity; and (iii) by comparing the theoretical dispersions of the refractive indices calculated within the scissor procedure to experimental ones, the rigid band gap (without polaron effects) of SLN at 0 K is estimated to (4.8 ± 0.1) eV, and this value confirms a previous one (4.7 eV) directly obtained by GW calculation [17]; (iv) finally, the good agreement obtained for the dispersions through our corrected GGA method suggests to use it systematically for any insulator in which the electron–phonon coupling is strong enough to give polaron levels in the band gap, or otherwise to use the GW method, or preferably both.

References

[1] A.M. Glass, D. Yon der Linde, D.H. Auston, T.J. Negran, J. Electron. Mater. 4 (1975) 915.
[2] R.S. Weis, T.K. Gaylord, Appl. Phys. A 37 (1985) 191.
[3] P. Günter, J.P. Huignard, Photorefractive Mater. Appl. 1 (Springer Ser. Opt. Sci.) 113 (2006).
[4] P. Günter, J.P. Huignard, Photorefractive Mater. Appl. 2 (Springer Ser. Opt. Sci.) 114 (2007).
[5] P. Günter, J.P. Huignard, Photorefractive Mater. Appl. 3 (Springer Ser. Opt. Sci.) 115 (2007).
[6] T. Volk, M. Wöhlecke, Lithium Niobate, Defects, Photorefraction Ferroelectric Switching Springer Ser. Mater. Sci. 113 (2008).
[7] P. Hohenberg, W. Kohn, Phys. Rev. B 136 (1964) 864.
[8] I. Inbar, R.E. Cohen, Phys. Rev. B 53 (1996) 1193.
[9] S. Kohiki, M. Arai, H. Yoshikawa, S. Fukushima, Phys. Rev. B 57 (1998) 14572.
[10] V. Caciuc, A.V. Postnikov, G. Brostel, Phys. Rev. B 61 (2000) 8806.
[11] K. Parlinski, Z.Q. Li, Y. Kawazoe, Phys. Rev. B 61 (2000) 272.
[12] W.Y. Ching, Gu. Zong-Quan, Xu. Yong-Nian, Phys. Rev. B 50 (1994) 1992.
[13] M. Veithen, P. Ghosez, Phys. Rev. B 65 (2002) 214302.
[14] Qingkun Li, Biao Wang, C.H. Woo, Hai Wang, Rui Wang, J. Phys. Chem. Solids 68 (2007) 1336.
[15] H.H. Nahm, C.H. Park, Phys. Rev. B 78 (2008) 184108.
[16] W.G. Schmidt, M. Albrecht, S. Wippermann, S. Blankenburg, E. Rauls, F. Fuchs, C. Rödl, J. Furthmüller, A. Hermann, Phys. Rev. B 77 (2008) 035106.

[17] C. Thierfelder, S. Sanna, A. Schindlmayr, W.G. Schmidt, Phys. Status Solidi C 7 (2010) 362.
[18] H.A. Rahnamaye Aliabad, A. Iftikhar, Physica B 407 (2012) 368.
[19] M.T. Yin, M.L. Cohen, Phys. Rev. B 26 (1982) 5668.
[20] D.R. Hamann, Phys. Rev. Lett. 42 (1979) 662.
[21] R.W. Godby, M. Schluter, L.J. Sham, Phys. Rev. B 37 (1988) 10159.
[22] A. Dhar, A. Mansingh, J. Appl. Phys. 68 (1990) 5804.
[23] M. Fox, Optical Properties of Solids, Oxford university press, 2011.
[24] M. Lanoo, M. Schullüter, L.J. Sham, Phys. Rev. B 32 (1984) 3890.
[25] Z. Feng, H. Hu, S. Cui, W. Wang, C. Lu, Cent. Eur. J. Phys. 7 (2009) 786.
[26] U. Scharb, K. Betzler, Phys. Rev. B 48 (1993) 15613.
[27] D.H. Jundt, M.M. Fejer, R.L. Byer, IEEE J. Quant. Electron. 26 (1990) 135.
[28] O.K. Anderssen, Phys. Rev. B 12 (1975) 3060.
[29] S. Wie, H. Krakauer, ibid. 11, 1985, 1200.
[30] M. Peterson, F. Wanger, L. Hufnagel, M. Scheffler, P. Blaha, K. Schwars, Comput. Phys. Commun. 126 (2000) 294.
[31] P. Blaha, K. Schwarz, G.D. Kvasnicka, J. Luitz, *WIEN2k* an augmented plane wave + local orbitals program for calculating crystal properties, Karlheinz Schwarz, Techn. Universität Wien, Austria, 2001.
[32] W. Kohn, L.J. Sham, Phys. Rev. A 140 (1965) 1133.
[33] J.P. Perdew, S. Burke, M. Ernzerhof, Phys. Rev. Lett. 77 (1996) 3865.
[34] H.J. Monkhorst, J.D. Pack, Phys. Rev. B 13 (1976) 5188.
[35] S.C. Abrahams, J.M. Reddy, J.L. Bernstein, J. Phys. Chem. Solids 27 (1966). 997, 1013, 1019.
[36] L.J. Sham, M. Schlüter, Phys. Rev. Lett. 51 (1983) 1888.
[37] S. Wey, A. Zunger, Phys. Rev. B 32 (1984) 3890.
[38] E.A. Albanesi, W.L. Lambercht, B. Seggal, J. Vac. Sci. Technol. B 12 (1994) 2470.
[39] R. Laskowski, N.E. Christensn, G. Santi, C. Ambrosch-Draxal, Phys. Rev. B 72 (2005) 035204.
[40] L. Makinistian, E.A. Albanesi, J. Phys.: Condens. Matter 19 (2007) 186211.
[41] Z.H. Levine, D.C. Allan, Phys. Rev. Lett. 63 (1989) 1719.
[42] F. Nastos, B. Olejnik, K. Schwarz, J.E. Sipe, Phys. Rev. B 72 (2005) 045223.
[43] C. Ambrosch-Draxl, J.O. Sofo, Comput. Phys. Commun. 175 (2006).
[44] Xu, Shang-Peng Gao, Inter J. Hyd. Energy 37 (2012) 11072.
[45] Yuan, P.S. Yadav, R.K. Yadav, S. Agrawal, B.K. Agrawal, Prog. Cryst. Growth Character. Mater. 52 (2006) 10–14.
[46] O.F. Schirmer, M. Imlau, C. Merschjann, B. Schoke, J. Phys.: Condens. Matter 21 (2009) 123201.